Control of the Transmembrane Orientation and Interhelical Interactions within Membranes by Hydrophobic Helix Length[†]

Jianhua Ren, Scott Lew, Jiyao Wang, and Erwin London*

Department of Biochemistry and Cell Biology and Department of Chemistry, State University of New York at Stony Brook, Stony Brook, New York 11794-5215

Received December 15, 1998; Revised Manuscript Received March 22, 1999

ABSTRACT: We examined the effect of the length of the hydrophobic core of Lys-flanked poly(Leu) peptides on their behavior when inserted into model membranes. Peptide structure and membrane location were assessed by the fluorescence emission λ_{max} of a Trp residue in the center of the peptide sequence, the quenching of Trp fluorescence by nitroxide-labeled lipids (parallax analysis), and circular dichroism. Peptides in which the hydrophobic core varied in length from 11 to 23 residues were found to be largely α-helical when inserted into the bilayer. In dioleoylphosphatidylcholine ($diC_{18:1}PC$) bilayers, a peptide with a 19-residue hydrophobic core exhibited highly blue-shifted fluorescence, an indication of Trp location in a nonpolar environment, and quenching localized the Trp to the bilayer center, an indication of transmembrane structure. A peptide with an 11-residue hydrophobic core exhibited emission that was red-shifted, suggesting a more polar Trp environment, and quenching showed the Trp was significantly displaced from the bilayer center, indicating that this peptide formed a nontransmembranous structure. A peptide with a 23-residue hydrophobic core gave somewhat red-shifted fluorescence, but quenching demonstrated the Trp was still close to the bilayer center, consistent with a transmembrane structure. Analogous behavior was observed when the behavior of individual peptides was examined in model membranes with various bilayer widths. Other experiments demonstrated that in $diC_{18:1}PC$ bilayers the dilution of the membrane concentration of the peptide with a 23-residue hydrophobic core resulted in a blue shift of fluorescence, suggesting the red-shifted fluorescence at higher peptide concentrations was due to helix oligomerization. The intermolecular self-quenching of rhodamine observed when the peptide was rhodamine-labeled, and the concentration dependence of self-quenching, supported this conclusion. These studies indicate that the mismatch between helix length and bilayer width can control membrane location, orientation, and helix−helix interactions, and thus may mismatch control both membrane protein folding and the interactions between membrane proteins.

The structural features regulating the behavior of membrane-inserted hydrophobic helices are only poorly understood. The ability of the helices to pack tightly (*1*, *2*), and the nature of the amino acid sequence (*3*−*7*), are important factors that influence hydrophobic helix behavior. In addition, since membrane proteins have transmembrane segments of various lengths, and because membrane thickness can be modulated in vivo (e.g., by cholesterol content), another important factor may be the relationship of the length of the hydrophobic sequence to the width of the bilayer (*8*−*10*).

Mismatch between the width of the lipid bilayer and length of the hydrophobic segments of a membrane-inserted protein is believed to have several consequences. A number of studies have proposed that mismatch will result in either a compression or expansion of the lipid bilayer width adjacent to the membrane surface, and/or binding selectivity for lipids of proper length at the membrane-facing surface of a transmembrane protein (*10*−*15*). These changes would allow lipid to cover the hydrophobic surface of the lipid. Experimentally, significant changes in lipid structure due to mismatch have been detected in some systems (*14*), but at least for the Ca^{2+}ATPase of sarcoplasmic reticulum, no lipid length binding selectivity has been observed (*15*).

Mismatch also can result in a change in protein structure. Several studies have shown that membrane thickness can affect the activity of transmembrane proteins (*15*−*18*). One explanation for activity changes is that they result in changes in protein conformation that result in a match to bilayer width (*15*−*17*). It has also been suggested that self-association of membrane proteins within the bilayer may be affected by mismatch (*8*, *9*, *12*, *15*), although only weak effects were found for bacteriorhodopsin aggregation when the bilayer width was varied (*19*). A final consequence of mismatch may be that in membranes with lipid domains with different thicknesses there may be sorting of the proteins into the domains that minimize mismatch (*20*, *21*).

In this report, the effect of varying helix length on both the membrane location and self-association of hydrophobic helices has been examined using helix-forming Lys-flanked poly(Leu) (pLeu) peptides with a Trp residue at the center of the Leu sequence (*8*, *9*, *22*). In agreement with our previous study in which bilayer width was varied with a fixed length peptide (*8*), it was found that helices that are too short to span the bilayer are located closer to the bilayer surface

[†] This work was supported by NIH Grant GM 48596.

10.1021/bi982942a CCC: $18.00
Published on Web 04/15/1999

than transmembrane helices. Intriguingly, it is now found that peptides longer than necessary for spanning the bilayer remain transmembranous but appear to self-associate much more strongly than peptides with a length that matches bilayer width. A model for how the length of the hydrophobic peptide segment regulates helix behavior is described.

EXPERIMENTAL PROCEDURES

Materials. Peptides $K_2GL_5WL_5K_2A$ (pLeu11), $K_2GL_7WL_7K_2A$ (pLeu15), $K_2GL_9WL_9K_2A$ (pLeu19), $K_2L_{10}WL_{10}K_2A$ (pLeu21), and $K_2GL_{11}WL_{11}K_2A$ (pLeu23) were purchased from Research Genetics (Huntsville, AL). The peptides all had acetylated N-termini and amide-blocked C-termini. Phosphatidylcholines (PCs, 1,2-diacyl-*sn*-glycero-3-phosphocholines), diC14:1Δ9c PC [dimyristoleoyl-PC (DMoPC)], di16:1Δ9c PC [dipalmitoleoyl-PC (DPoPC)], di18:1Δ9c PC [dioleoyl-PC (DOPC)], di20:1Δllc PC [dieicosenoyl-PC (DEiPC)], di22:1Δ13c PC [dierucoyl-PC (DEuPC)], di24:1Δ15c PC [dinervonoyl-PC (DNPC)], 5(12)SLPC, 1-palmitoyl-2-[5(12)-doxyl]stearoyl-PC, and TempoPC [1-palmitoyl-2-oleoyl-*sn*-glycero-3-[4-[*N*,*N*-dimethyl-*N*-(2-hydroxyethyl)ammonium]]-2,2,6,6-tetramethylpiperidine-1-oxyl] were purchased from Avanti Polar Lipids, Inc. (Alabaster, AL). Cholesterol was from Aldrich (St. Louis, MO). Peptides were purified as described previously, and lipid and peptide purities were assessed as previously described (*8*).

Rhodamine Labeling and Purification of Labeled Peptides. To label pLeu peptides with rhodamine, 2 mg of 10% rhodamine sulfonyl chloride adsorbed on Celite (Molecular Probes, Eugene, OR) was suspended in 500 μL of 50 mM sodium carbonate (pH 9.2). This was mixed with 500 μL of purified pLeu peptide dissolved in ethanol. After being mixed overnight, the sample was subjected to high-speed centrifugation for 1 min to pellet the Celite, and then the labeled peptide was purified by HPLC using the same procedures that were used for unlabeled peptides. The HPLC of the labeled peptides showed a series of closely spaced peaks. MALDI-TOF mass spectrometry (Center for Analysis and Synthesis of Macromolecules, State University of New York at Stony Brook) was performed to determine the molecular weight of the species in each peak, and thus the degree of labeling. The overall fraction of labeled molecules was close to half, with the various singly labeled species at concentrations higher than those of doubly labeled species. The peaks corresponding to various monolabeled species were pooled to conserve materials. (Control fluorescence experiments with pure monolabeled species gave results similar to those for this mixture.)

Sample Preparation. Model membrane samples were prepared by ethanol dilution (*8*). The desired mixtures of lipids and peptide were dried first under nitrogen and then for 1 h under high vacuum. For ethanol dilution vesicles, 10 μL of 100% ethanol was added to dissolve the samples (20 μL in the experiments in which lipid concentration was varied and Trp fluorescence was measured). Then 600 μL of 12 mM mixed sodium and potassium phosphate, 137 mM NaCl, and 3 mM KCl (pH 7.4) (PBS) was added and the mixture vortexed to disperse the lipid/peptide mixture. Unless otherwise noted, the final phospholipid concentration was 500 μM and the peptide concentration was 2 μM. Previous control experiments demonstrated that the small amount of residual ethanol has no effect on peptide behavior (*8*).

Fluorescence and Circular Dichroism Measurements. Tryptophan fluorescence was measured at room temperature on a SPEX τ2 Fluorolog spectrofluorometer operating in the steady state mode. Emission spectra were measured in a semimicro quartz cuvette (1 cm excitation path length and 4 mm emission path length) with excitation at 280 nm, generally using a 2.5 mm excitation slit and 5 mm emission slit. The fluorescence of background samples without peptide was measured and subtracted from reported data.

Circular dichroism (CD) spectra were recorded using a JASCO J-715 CD spectrometer as previously described (*8*). Samples were prepared in 1/10 PBS [as in the previous report (*8*), although unnoted in the text] to reduce the amount of interference with low-wavelength measurements. Control experiments with full-strength PBS gave similar results, except that readings could not be taken below 200 nm.

Measurement of the Extent of Rhodamine Self-Quenching. To measure the extent of rhodamine self-quenching, samples were prepared as described above, except for the concentrations of peptides and lipid. One set of samples (*F* samples) contained 0.1 μM labeled peptide in 5, 100, or 250 μM DOPC. The second set (F_o samples) contained 0.1 μM labeled peptide and 0.5 μM unlabeled peptide in 5, 100, or 250 μM DOPC. Fluorescence was measured at an excitation wavelength of 555 nm and emission wavelength of 585 nm.

Fluorescence Quenching Measurements. For fluorescence quenching experiments, vesicles were prepared from DOPC or mixtures of DOPC and 15% quencher (nitroxide)-labeled lipid (either TempoPC, 5SLPC, or 12SLPC) as previously described (*8*). Duplicate samples were prepared similarly as described above except that after drying they were dissolved with 20 μL of ethanol and dispersed in 980 μL of 10 mM sodium phosphate and 150 mM NaCl (pH 7.5−7.6) to give a final peptide concentration of 2 μM and a lipid concentration of 200 μM. Emission intensity was recorded at room temperature at the wavelength of maximum emission. Trp depths (z_{cf}, distance from the bilayer center) were determined from fluorescence intensities using parallax analysis as previously described (*8*).

RESULTS

Effect of Bilayer Width on the Wavelength of Trp Emission from pLeu Peptides of Various Lengths. To examine the effect of hydrophobic helix length on behavior, Lys_2-flanked peptides with different length pLeu sequences were examined. The peptides that were examined were pLeu11, pLeu15, pLeu19, pLeu21, and pLeu23, where the number designates the total number of hydrophobic residues in each peptide (there are also three flanking residues on each side of the hydrophobic sequence). The λ_{max} of the fluorescence of a single Trp in the center of the pLeu sequence (and thus in the center of the peptide sequence) was used to evaluate the apparent polarity of the Trp environment within the bilayer (*8*). For example, the closer a Trp group is to the bilayer surface, the progressively higher its λ_{max} value (i.e., the less strongly blue-shifted its fluorescence).[1]

[1] It should be noted that solvent relaxation effects, polarization artifacts, and local sequence can complicate the interpretation of λ_{max}, so it should only be considered an approximate measure of local polarity.

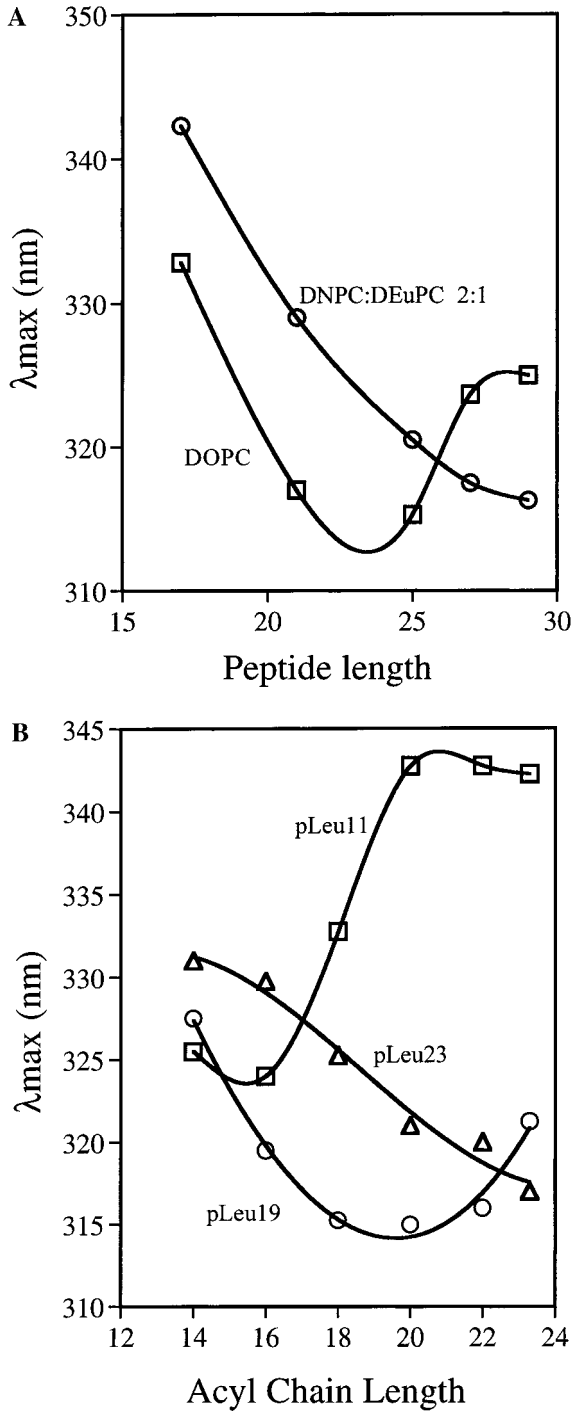

FIGURE 1: Effect of peptide length and lipid bilayer width on the λ_{max} of Trp fluorescence emission in pLeu peptides. (A) Effect of peptide length. The *x*-axis gives the total number of amino acid residues in the peptide: (□) peptides incorporated into DOPC vesicles and (○) samples incorporated into DNPC/DEuPC (2/1) vesicles. Samples contained 2 μM peptide incorporated into 500 μM lipid vesicles (pH 7.4). (B) Effect of bilayer width. The *x*-axis gives the number of carbon atoms in the fatty acyl chains of the lipids that were used: (□) pLeu11, (○) pLeu19, and (△) pLeu23. Samples contained 2 μM peptide incorporated into 500 μM lipid vesicles (pH 7.4). The λ_{max} values shown are the averages of duplicate experiments and were generally reproducible to within 1 nm in this and the following figures.

Figure 1A shows that the Trp fluorescence of pLeu peptides incorporated into DOPC ($diC_{18:1}PC$) vesicles is dependent on peptide length. Trp emission is most blue-shifted for pLeu15 and pLeu19, which have hydrophobic lengths that come close to matching the width of the hydrophobic core of DOPC (see the Discussion). We have shown previously that this highly blue-shifted Trp fluorescence is indicative of a transmembrane orientation (*8*). Peptides shorter or longer than pLeu15 and pLeu19 give more red-shifted fluorescence, suggesting that their Trp residue is in an environment more polar than that for pLeu15 and pLeu19.

The relationship between peptide length and Trp fluorescence was also examined in wider bilayers, composed of a 2/1 (moles per mole) DNPC/DEuPC ($diC_{24:1}PC/diC_{22:1}PC$) mixture which has an average length of 23.3 carbon atom acyl chains,[2] in contrast to 18 carbon atoms for DOPC (Figure 1A). In the DNPC/DEuPC bilayers, pLeu23, which has the longest hydrophobic sequence examined, exhibited the most blue-shifted fluorescence. Since of all the peptides studied, the length of the hydrophobic sequence of this peptide is closest to the width of the hydrophobic core of the 2/1 DNPC/DEuPC bilayers, it appears to be a general rule that the most blue-shifted fluorescence is observed where the length of the helix formed by the hydrophobic segment of the peptide comes close to matching bilayer width (see the Discussion).

This conclusion is supported by the complementary experiment in which the effect of varying bilayer width upon peptide λ_{max} was examined (Figure 1B). Bilayer width was varied by incorporating the peptides in model membranes composed of phospholipids with various acyl chain lengths. The fluorescence of pLeu11 was most blue-shifted in the thinnest bilayers DMoPC ($diC_{14:1}PC$) and DPoPC ($diC_{16:1}PC$),[3] that of pLeu19 most blue-shifted in intermediate width bilayers, and that of pLeu23 most blue-shifted fluorescence in the widest bilayers. Thus, the linkage of the blue shift of fluorescence to the degree of match between bilayer width and helix length is observed over a significant range of lipid widths and peptide lengths.

Fluorescence Quenching Analysis of pLeu Peptide Trp Depth. To more directly evaluate membrane location, fluorescence quenching by nitroxide (spin)-labeled phospholipids was measured. In these experiments, the depth of a fluorophore (here Trp) is calculated [using parallax analysis (*8*)] from the ratio of its quenching by lipids carrying a fluorescence quenching nitroxide label at different depths. The lipids that were used carry either a shallow (TempoPC), intermediate depth (5SLPC), or deep (12SLPC) nitroxide group. We have previously shown that this method can give accurate depths of fluorescence residues in a wide variety of cases (see refs in ref *8*).

Table 1 shows there is strong quenching of pLeu11, pLeu19, and pLeu23 by lipids carrying a nitroxide group, as expected for membrane-inserted molecules. Using the quenching data to calculate depth shows the Trp residue for

[2] A mixture of DNPC and DEuPC was used because pure DNPC has a melting temperature of 24 °C (*15*), and we wished to maintain a fluid bilayer in all experiments.

[3] The results of such experiments in thin bilayers, such as those formed by DMoPC, are difficult to interpret because even at the bilayer center a Trp is significantly closer to the surface than it would be when at the center of a thicker bilayer, and thus may not exhibit a λ_{max} as blue-shifted as that seen in the latter case. This may explain why pLeu11 gave slightly more blue-shifted fluorescence in DPoPC than in DMoPC (Figure 1B), although the length of its hydrophobic sequence is closer to that of DMoPC (see the Discussion).

Table 1: Fluorescence Quenching of Vesicle-Inserted pLeu Peptides by Nitroxide (Spin)-Labeled Lipids[a]

peptide	$F_{TempoPC}/F_o$	F_{5SLPC}/F_o	F_{12SLPC}/F_o	z_{cf} (Å)	λ_{max} (nm)
pLeu11	0.53 ± 0.019	0.40 ± 0.045	0.21 ± 0.015	5.4, 5.6	336
pLeu19	0.67 ± 0.026	0.59 ± 0.020	0.085 ± 0.008	0.2, 0.6	317
pLeu23	0.68 ± 0.055	0.67 ± 0.13	0.15 ± 0.036	1.7, 0.9	328

[a] F/F_o is the ratio of Trp fluorescence intensity in samples containing DOPC with 15 mol % active nitroxide-labeled lipid to that in 100% DOPC. Calculation of z_{cf}, the distance of the fluorescence group from the bilayer center, was performed using the F/F_o values from the 5SLPC/12SLPC pair using the parallax equation for residues close to the bilayer center (*8*). Average F/F_o values from four samples (two experiments with duplicates) and the standard deviation are shown. λ_{max} is the emission λ_{max}. The z_{cf} values calculated for individual experiments are shown. The nitroxide lipids that were used have 16 and 18 carbon acyl chains, and so do not significantly alter DOPC bilayer width.

pLeu19 is at the bilayer center (z_{cf}, the distance from the bilayer center, was <1 Å).[4] Since this residue is at the center of the Leu sequence, and the charged flanking Lys groups must be near the surface,[5] this confirms that pLeu19 is transmembranous. This conclusion is strongly supported both by the experimentally determined depths of Trp groups when they are moved to different positions in the pLeu sequence and by other studies with similar pLeu peptides (*8*, and references therein).

The depth of the Trp of pLeu11 in nitroxide lipid/DOPC is significantly shorter than that of pLeu19 (average z_{cf} = 5.5 Å). Since pLeu11 also exhibits strongly red-shifted fluorescence, it is likely most pLeu11 molecules are in a nontransmembranous conformation. For flanking Lys residues to remain at the membrane surface, this conformation would have to be closer to the bilayer surface than the bilayer center. However, it should be noted that some fraction of pLeu11 molecules are likely to be in a transmembrane form in DOPC bilayers.

This inference is based on two observations. First, we previously found that transmembrane and nontransmembrane conformations can be in equilibrium when mismatch is not extreme (*8*). Second, in bilayers that are wider than DOPC, the fluorescence of the pLeu11 Trp is even more highly red-shifted than in DOPC (Figure 1B), giving a limiting λ_{max} value of 342 nm. This observation is consistent with the shift being more extreme when the entire population of peptides is nontransmembranous. Furthermore, since a value of 342 nm should correspond to a Trp at the membrane surface (*8*), it is likely that the nontransmembrane conformation formed when pLeu11 is too short to span the bilayer is indeed close to the bilayer surface.

In contrast, the apparent depth of the Trp of pLeu23 in DOPC was only slightly less than that of pLeu19 (average z_{cf} = 1.3 Å), strongly suggesting that the large majority of pLeu23 molecules remain transmembranous, despite the red shift of its Trp fluorescence.[6] Together, these experiments suggest there is some difference between the behavior of pLeu23 and that of both pLeu11 and pLeu19 (see below).

Secondary Structure of pLeu Peptides. One possibility for the differences in the behavior of the peptides noted above is that they are related to secondary structure. In general, pLeu peptides form α-helices (*8*, *9*, *23*, *24*). Nevertheless, it is possible that they exhibit differences in secondary structure under some conditions. However, the CD spectra in Figure 2 show that spectral shapes and intensities for the shortest (pLeu11), intermediate (pLeu19), and longest (pLeu23) peptides are very similar. The intensity of ellipticity and spectral shapes (with minima near 208 and 222 nm) correspond to strongly α-helical molecules (*8*). It appears that pLeu11 may have a slightly higher fractional α-helix content than pLeu19 and pLeu 23. The CD spectra of the peptides are also very similar in thin (DMoPC), intermediate (DOPC), or thick [2/1 (moles per mole) DNPC/DEuPC] model membranes (Figure 2). Therefore, secondary structure is not strongly influenced by bilayer width. These observations imply that the differences in Trp depth and environment when peptide length or bilayer width is varied are not due to secondary structure differences.

Membrane Concentration Dependence of pLeu Fluorescence. Another possible explanation for the difference in the behavior of pLeu19 and pLeu23 is that they have a different degree of self-association within the bilayer. The overall weaker quenching of pLeu23 relative to that of pLeu19 is consistent with self-association of pLeu23 because that would shield Trp from the lipid acyl chains, and thus from quenching by the lipid-attached nitroxide. If the environment in the center of a peptide oligomer is more polar than that formed by lipid, then self-association might also explain why pLeu23 Trp fluorescence is somewhat red-shifted.

To examine the possibility of helix self-association, the dependence of Trp fluorescence on the concentration of peptide within the bilayer was determined. This was varied by changing the lipid concentration at a fixed total peptide concentration. As shown in Figure 3A, the effect of membrane concentration of the peptide upon fluorescence λ_{max} depends on both lipid and peptide length. The pLeu19 peptide in DOPC exhibits no concentration dependence, whereas the pLeu23 peptide exhibits a progressive blue shift as it is diluted in the DOPC bilayer. This concentration dependence can best be explained by assuming the more red-shifted species is an oligomer in the bilayer that dissociates into a less oligomerized species in which the Trp environment is similar to that when peptide length and bilayer width match (e.g., for pLeu19 in DOPC). This conclusion is supported by the behavior of pLeu23 incorporated into 2/1 DNPC/DEuPC vesicles, in which there is very little mismatch. This abolished most of the concentration dependence of λ_{max}.[7]

Cholesterol can affect the behavior of membrane-inserted helices, apparently via the increase in bilayer width in its

[4] We did not measure the extent of fluorescence quenching in bilayers other than DOPC because a change in bilayer width can alter apparent depth. Specifically, the amount of quenching from the leaflet of the bilayer opposite of the one in which the fluorophore is located will be strongly dependent on bilayer width. In addition, the exact depth of the nitroxide group has only been well calibrated in DOPC (*8*).

[5] The pK_a of the flanking Lys groups on this peptide, about 10.5, is close to that expected for Lys in aqueous solution, indicating that Lys is located outside the bilayer (data not shown).

[6] Since, as discussed below, the Trp in pLeu23 may be shielded from lipid by self-association, and because in such a case the depth derived from parallax analysis may be only an upper limit to the actual Trp depth (calculation not shown), it is possible that the Trp in pLeu23 is as deeply located as in pLeu19.

[7] Interestingly, no dependence of λ_{max} upon lipid concentration was observed for pLeu11. This is not surprising if the red shift in its Trp fluorescence is due to a surface location, rather than to oligomerization.

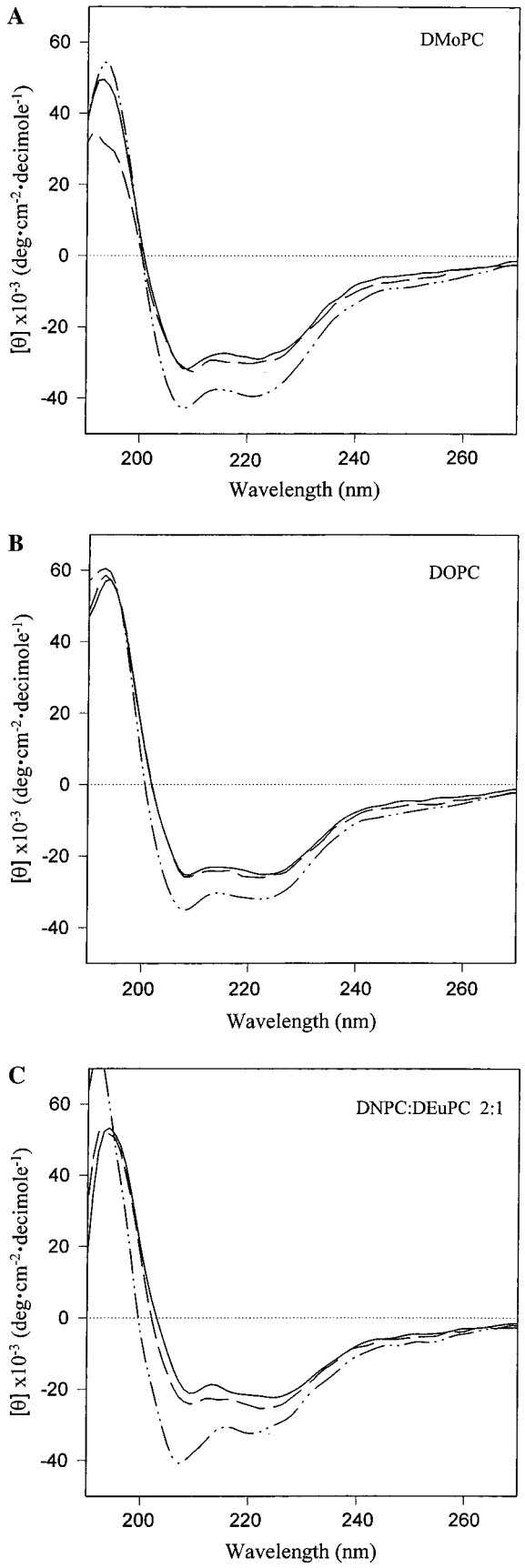

FIGURE 2: Low-UV circular dichroism spectra of pLeu peptides in bilayers with different widths. Peptides were incorporated into (A) DMoPC ($diC_{14:1}PC$), (B) DOPC ($diC_{18:1}PC$), or (C) 2/1 DNPC/DEuPC ($diC_{24:1}PC/diC_{22:1}PC$) vesicles: (−••−) pLeu11, (− − −) pLeu19, and (—) pLeu23. In these experiments, the peptide concentration was 2.5 μM and the lipid concentration 200 μM.

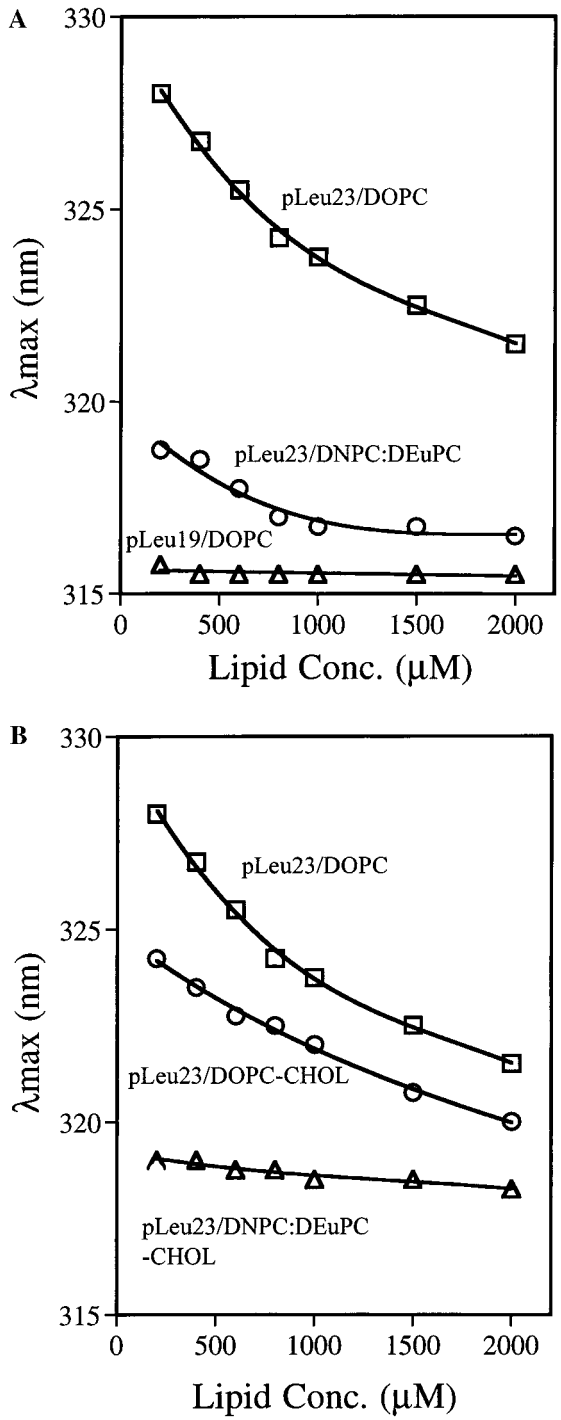

FIGURE 3: Effect of pLeu peptide concentration within the membrane bilayer upon the λ_{max} of Trp fluorescence emission: (A) (□) pLeu23 in DOPC vesicles, (△) pLeu19 in DOPC vesicles, and (○) pLeu23 in 2/1 DNPC/DEuPC vesicles and (B) (□) pLeu23 in DOPC vesicles, (○) pLeu23 in 7/3 DOPC/cholesterol vesicles, and (△) pLeu23 in 4.66/2.33/3 DNPC/DEuPC/cholesterol vesicles. The concentration of peptide in these samples was 2 μM. The lipid concentration was varied. Other sample conditions are as described in the legend of Figure 1.

presence (*8*, *9*). Therefore, how cholesterol influences the dependence of fluorescence λ_{max} upon the membrane concentration of peptide was also examined. In DOPC bilayers containing cholesterol (Figure 3B), pLeu23 exhibited both more blue-shifted fluorescence and a somewhat reduced dependence of λ_{max} on lipid concentration relative to corresponding samples lacking cholesterol (Figure 3A). This is

consistent with the prediction of an increased bilayer width (and thus less mismatch) in the presence of cholesterol (*8*).

In thicker, DNPC/DEuPC, bilayers, pLeu23 exhibited no dependence of λ_{max} on lipid concentration in samples containing cholesterol and exhibited a slight red shift relative to samples lacking cholesterol. This is consistent with DNPC/DEuPC bilayers switching from being slightly thinner than the length of the hydrophobic helix of pLeu23 to being slightly thicker than the hydrophobic helix length upon the inclusion of cholesterol.

Detection of Interhelical Association by Fluorescence Self-Quenching. To confirm that pLeu23 had an increased tendency for interhelical interactions, helix self-association was also assessed via rhodamine self-quenching in rhodamine-labeled peptides. In this assay, association between polypeptides results in self-quenching of rhodamine groups that are close to each other (*25*−*27*). The amount of self-quenching is estimated from the effect of the inclusion of an excess of unlabeled pLeu helices on rhodamine fluorescence. In the presence of a sufficient excess of unlabeled peptides, there should be no more than one labeled molecule per oligomer, abolishing self-quenching. In contrast, addition of an unlabeled peptide should have no effect on rhodamine fluorescence of peptides that are in the monomeric form. One advantage of this analysis is that it should not be affected by any self-quenching due to helices in close proximity simply due to their random lateral distribution in the membrane. This is true because the inclusion of unlabeled molecules should not significantly affect the distance between randomly distributed rhodamine-labeled molecules.

Figure 4 shows the effect of membrane concentration on the self-quenching of rhodamine-labeled pLeu19 and pLeu23. Notice that the fluorescence values are normalized to fluorescence in the presence of a 5-fold excess of unlabeled peptide. It appears that there is some degree of oligomerization of both pLeu19 and pLeu23. The tendency of pLeu19 to self-associate appears to be weaker than that on pLeu23, as indicated by the greater loss of pLeu19 self-quenching at high dilutions in the bilayer. With a peptide/lipid ratio of 2500/1, the self-quenching of pLeu19 appears to be largely eliminated.

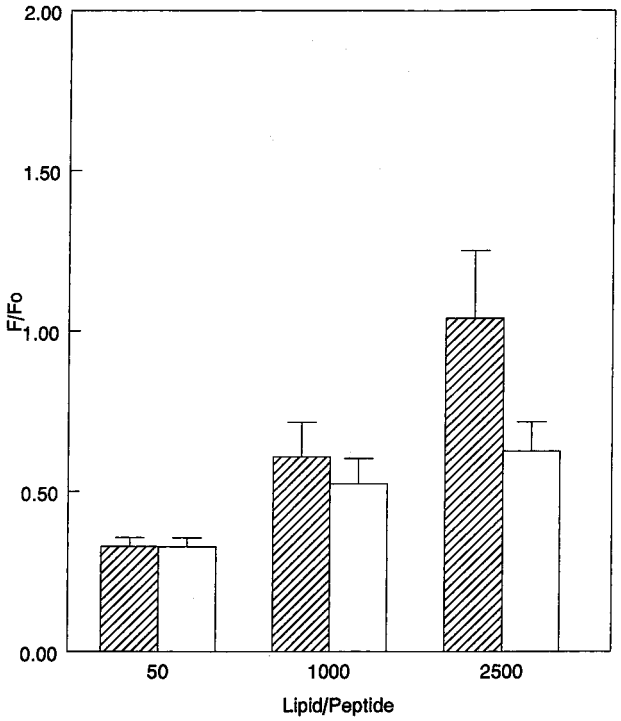

FIGURE 4: Degree of rhodamine self-quenching of rhodamine-labeled pLeu peptides: (striped bars) pLeu19 and (white bars) pLeu23. The average and standard deviation of three experiments are shown at three different lipid/peptide ratios (moles per mole). F/F_o is the ratio of fluorescence in samples containing 0.1 μM peptide inserted into DOPC vesicles (pH 7.4) to that in similar samples containing labeled 0.1 μM membrane-inserted peptide mixed with a 5-fold molar excess of unlabeled peptide. (Because this 5-fold excess may not be enough to totally abolish self-quenching, these values may represent an upper limit to F/F_o.) The *x*-axis gives the ratio of lipid to rhodamine-labeled protein.

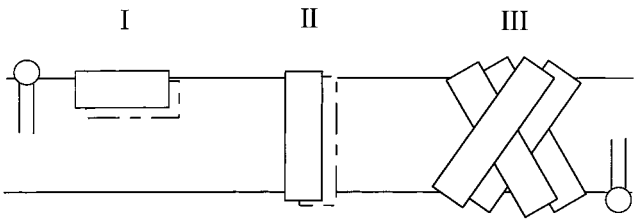

FIGURE 5: Schematic illustration of the effect of mismatch on the behavior of hydrophobic helices: (case I) helix too short to span the bilayer, (case II) helix length matches bilayer width, and (case III) helix longer than necessary to span the bilayer. Notice that the extent of helix self-association is greatest in case III, and uncertain in cases I and II as shown by the dotted outlines. The absolute degree of self-association in case III is not known. Any effects of the helices on lipid bilayer structure are not illustrated.

DISCUSSION

Helix Length−*Bilayer Width Mismatch Determines Helix Behavior: Conditions under Which Helix Length Matches Hydrophobic Bilayer Width.* This study shows that the mismatch arising from varying the helix length has consequences for two important aspects of helix behavior, namely, helix location and helix−helix interactions. The results suggest that when bilayer width is close to matching the length of the hydrophobic sequence, a transmembrane structure forms in which the fluorescence of a Trp at the bilayer center is highly blue-shifted (Figure 5).

To demonstrate that this corresponds to the case when there is very little mismatch, the values of the peptide length and the width of the hydrophobic part of the bilayer should be compared. Peptide pLeu19 has un uncharged sequence of 20 residues (including the Gly at position 3), which in helical form will be very close to 30 Å long (Table 2). The sequence of pLeu11 has a 12-residue uncharged sequence, which could yield an 18 Å long hydrophobic helix, and analogously for pLeu23, the hydrophobic helix length would be 36 Å. To calculate bilayer width, the estimate for the hydrophobic core width of DOPC close to 28 Å, in the fully hydrated form (*9*, *28*, *29*), can be combined with the observation that bilayer width increases by about 1.8 Å per increase of one fatty acyl chain carbon atom (*30*) (0.9 Å in each leaflet). This gives a calculated hydrocarbon core width of 21 Å for DMoPC, 24.5 Å for DPoPC, and 37.5 Å for the 2/1 DNPC/DEuPC mixture (Table 2). Thus, the observations that peptide pLeu19 (30 Å) gave the most blue-shifted fluorescence in DOPC (28 Å), pLeu11 (18 Å) in DMoPC and DPoPC (average of 23 Å), and pLeu23 (36 Å) in 2/1 DNPC/DEuPC (37.5 Å) indicate that a near match between

Table 2: Dimensions of Peptides and Bilayers

peptide	no. of hydrophobic residues	total no. of residues	approximate length of the hydrophobic helix (Å)[a]
pLeu11	11	17	18
pLeu15	15	21	24
pLeu19	19	25	30
pLeu21	21	27	33
pLeu23	23	29	36

lipid	width of the hydrocarbon core (Å)[b]
$diC_{14:1}PC$	21
$diC_{16:1}PC$	24.5
$diC_{18:1}PC$	28
$diC_{20:1}PC$	31.5
$diC_{22:1}PC$	35
$diC_{24:1}PC/diC_{22:1}PC$ (2/1)	37.5

[a] Including Gly bordering the hydrophobic sequence. [b] Based on a 28 Å hydrocarbon core for $diC_{18:1}PC$, and an additional 1.8 Å width per additional fatty acyl carbon atom.

bilayer width and peptide length is involved.[3] Therefore, the difference between lipid width and helix length is a much more important determinant of helix behavior than the absolute values of bilayer width or helix length, in agreement with previous studies (*31*).

Consequences of Mismatch When a Helix Is Too Short To Span the Bilayer. The results in this study, combined with those of our previous report (*8*), demonstrate that when a hydrophobic helix is too short to span the bilayer, the helix moves to a nontransmembrane orientation close to the bilayer surface (Figure 5). Presumably, the ability of the lipids to undergo bilayer thinning is too limited to fully accommodate a transmembrane orientation for the 12-residue uncharged sequence in pLeu11.

Webb et al. (*9*) also found that when the mismatch between a short peptide and the bilayer width was extreme the transmembrane conformation was lost. However, they found under such conditions that the peptide failed to associate with the bilayer, apparently aggregating in solution (*9*). The difference between our results and those of Webb et al. appears to be due to the different procedures that were used for sample preparation. We found that pLeu11 was not membrane incorporated when samples were prepared by the co-drying/sonication procedure of Webb et al., although it was incorporated with the rapid dilution procedure used in this study. [This was shown by the observation that there was no quenching of pLeu11 Trp fluorescence by nitroxide-labeled lipids incorporated into DNPC-containing vesicles made by sonication, but quenching in such vesicles was as almost strong as in DOPC-containing bilayers when using the dilution procedure (data not shown)[8].] No matter which of these behaviors is considered, it is clear the transmembrane orientation of a short hydrophobic helix such as pLeu11 is clearly unstable, at least in the absence of long flanking hydrophilic sequences.

[8] We previously demonstrated that the presence of ethanol does not affect the results of these experiments (*8*). In addition, control experiments were performed with samples of pLeu23 incorporated both in multilamellar DOPC vesicles and in small unilamellar DOPC vesicles prepared by sonication (*8*). The dependence of λ_{max} upon lipid concentration in these samples was very similar to that in the vesicles prepared in the presence of ethanol (data not shown).

Consequences of Mismatch When a Helix Is Longer Than Needed To Span the Bilayer: Increased Interhelical Associations and Implications for Membrane Protein Folding. Another important observation in this report was that helices longer than necessary to span the lipid bilayer exhibit increased levels of self-association (Figure 5). This was shown both by the dependence of λ_{max} and that of rhodamine self-quenching upon the membrane concentration of such peptides. This dependence was much stronger for pLeu23 than for pLeu19, suggesting the former has a stronger tendency to oligomerize. On the other hand, self-quenching suggested a significant degree of oligomerization of pLeu19 except when very dilute within the bilayer. One possibility is that pLeu19 tends to form a much smaller oligomer than does pLeu23. In a small oligomer, the Trp residue might remain lipid-exposed, and thus have the same λ_{max} as in a monomer. This would explain the lack of a concentration dependence of the pLeu19 λ_{max}. In any case, more precise analysis of interhelical interaction will be an important goal of future studies.

One question raised by these studies is why the strongest interactions between helices occur when the hydrophobic sequence is longer than necessary to span the bilayer. One possibility is that by minimizing the area of the lipid−peptide contact, interhelical interactions minimize lipid perturbation (*12*, *31*). Another possibility is that the consequences of this type of mismatch for interhelical packing may be important. The studies of Engelman and colleagues have demonstrated that tight interhelix packing drives the strong dimeric self-association of the transmembrane segment of glycophorin (*1*, *32*). The tilted structure that would be likely for helices that exceed the length needed to span the bilayer should assist tight packing (Figure 5). In this regard, it is noteworthy that membrane proteins with multiple helical segments tend to have tilted and tightly packed transmembrane helices (*33*, *34*).

Lipid composition may also play a role in regulating interhelical interactions and membrane protein folding. We previously found that the effects of the inclusion of physiological cholesterol levels in model membranes on helix behavior can be explained by the effect of cholesterol on bilayer width (*8*). Combined with the observations of this study, these results suggest that the movement of a protein between a cholesterol-rich membrane domain forming a thick bilayer, and one that is cholesterol-poor and thin, could alter helix−helix association and/or dissociation. This is an interesting issue in view of the increasing body of evidence for coexisting membrane domains with different lipid compositions, and (apparently) different widths (*19*, *35*, *36*).

ACKNOWLEDGMENT

We thank Robert Kaiser and Steven O. Smith for helpful discussions.

REFERENCES

1. Lemmon, M. A., Flanagan, J. M., Treutlein, H. R., Zhang, J., and Engelman, D. M. (1992) *Biochemistry 31*, 12719−12725.
2. Cosson, P., and Bonifacio, J. S. (1992) *Science 258*, 659−662.
3. Liu, L. P., and Deber, C. M. (1997) *Biochemistry 36*, 5476−5482.

4. Chung, L. A., Lear, J. D., and DeGrado, W. F. (1992) *Biochemistry 31*, 6608−6616.
5. Chung, L. A., and Thompson, T. E. (1996) *Biochemistry 35*, 11343−11354.
6. Landolt-Marticorena, C., Williams, K. A., Deber, C. A., and Reithmeier, R. A. F. (1993) *J. Mol. Biol. 229*, 602−608.
7. Cosson, P., Lankford, S. P., Bonifacio, J. S., and Klausner, R. D. (1991) *Nature 351*, 414−416.
8. Ren, J., Lew, S., Wang, Z., and London, E. (1997) *Biochemistry 36*, 10213−10220.
9. Webb, R. J., East, J. M., Sharma, R. P., and Lee., A. G. (1998) *Biochemistry 37*, 673−679.
10. Haydon, D. A., Hendry, B. M., Levinson, S. R., and Requena, J. (1977) *Nature 268*, 356−358.
11. Killian, J. A., Salemink, I., de Panque, R. R., Lindblom, G., Koeppe, R. E., II, and Greathouse, D. V. (1996) *Biochemistry 35*, 1037−1045.
12. Mouritsen, O. G., and Bloom, M. (1984) *Biophys. J. 46*, 1241−1253.
13. Ashcroft, R. G., Coster, H. G. L., and Smith, J. R. (1977) *Nature 269*, 819−820.
14. de Planque, M. R. R., Greathouse, D. V., Koeppe, R. E., II, Schafer, H., Marsh, D., and Killian, J. A. (1998) *Biochemistry 37*, 9333−9345.
15. Caffrey, M., and Feigenson, G. W. (1981) *Biochemistry 20*, 1949−1961.
16. Johannsson, A., Keightley, C. A., Smith, G. A., Richards, C. D., Hesketh, T. R., and Metcalfe, J. C. (1981) *J. Biol. Chem. 256*, 1643−1650.
17. Mobashery, N., Nielsen, C., and Andersen, O. S. (1997) *FEBS Lett. 412*, 15−20.
18. Montecucco, C., Smith, G. A., Dabbeni-sala, F., Johannsson, A., Galante, Y. M., and Bisson, R. (1982) *FEBS Lett. 144*, 145−148.
19. Lewis, B. A, and Engelman, D. M. (1983) *J. Mol. Biol. 166*, 203−210.
20. Bretscher, M. S., and Munro, S. (1993) *Science 261*, 1280−1281.
21. Munro, S. (1995) *EMBO J. 14*, 4695−4704.
22. Bolen, E., and Holloway, P. (1990) *Biochemistry 29*, 9638−9643.
23. Davis, J. H., Clare, D. M., Hodges, R. S., and Bloom, M. (1983) *Biochemistry 22*, 5298−5305.
24. Zhang, Y.-P., Lewis, R. N. A. H., Hodges, R. S., and McElhaney, R. N. (1992b) *Biochemistry 31*, 11579−11588.
25. Chung, L. A. (1988) Ph.D. Thesis, State University of New York at Stony Brook, Stony Brook, NY.
26. Selwyn, J. E., and Steinfeld, J. I. (1972) *J. Phys. Chem. 76*, 762−774.
27. MacDonald, R. I. (1990) *J. Biol. Chem. 265*, 13533−13539.
28. Wiener, M. C., and White, S. H. (1992) *Biophys. J. 61*, 437−447.
29. Hristova, K., and White, S. H. (1998) *Biophys. J. 74*, 2419−2433.
30. Lewis, B. A., and Engelman, D. M. (1983) *J. Mol. Biol. 166*, 211−217.
31. Killian, J. A. (1998) *Biochim. Biophys. Acta 1376*, 401−416.
32. MacKenzie, K. R., Prestegard, J. H., and Engelman, D. M. (1997) *Science 276*, 131−133.
33. Bowie, J. U. (1997) *J. Mol. Biol. 272*, 780−789.
34. Kovacs, F. A., and Cross, T. A. (1997) *Biophys. J. 73*, 2511−2517.
35. Ahmed, S. N., Brown, D. A., and London, E. (1997) *Biochemistry 36*, 10944−10953.
36. Brown, D. A., and London, E. (1998) *J. Membr. Biol. 164*, 103−114.

BI982942A